Published in final edited form as:
*Osteoarthritis Cartilage*. 2011 August ; 19(8): 1011–1018. doi:10.1016/j.joca.2011.04.005.

# Complex Loading Affects Intervertebral Disc Mechanics and Biology

**B.A. Walter**[1,2], **C.L. Korecki**[1], **D. Purmessur**[1,2], **P.J. Roughley**[3], **A.J. Michalek**[1], and **J.C. Iatridis**[1,2]

[1] College of Engineering and Mathematical Sciences, University of Vermont, Burlington, VT, USA

[2] Orthopaedic Research Laboratories, Mount Sinai School of Medicine, New York, NY, USA

[3] Shriners Hospital for Children, Montreal, QC, Canada

## Abstract

**Background—**Complex loading develops in multiple spinal motions and in the case of hyperflexion is known to cause intervertebral disc (IVD) injury. Few studies have examined the interacting biologic and structural alterations associated with potentially injurious complex loading, which may be an important contributor to chronic progressive degeneration.

**Objective—**This study tested the hypothesis that low magnitudes of axial compression loading applied asymmetrically can induce IVD injury affecting cellular and structural responses in a large animal IVD ex-vivo model.

**Methods—**Bovine caudal IVDs were assigned to either a control or wedge group (15°) and placed in organ culture for 7 days under static 0.2 MPa load. IVD tissue and cellular responses were assessed through confined compression, qRT-PCR, histology and structural and compositional measurements, including western blot for aggrecan degradation products.

**Results—**Complex loading via asymmetric compression induced cell death, an increase in caspase-3 staining (apoptosis), a loss of aggrecan and an increase in aggregate modulus in the concave annulus fibrosis. While an up-regulation of MMP-1, ADAMTS4, IL-1β, and IL-6 mRNA, and a reduced aggregate modulus were induced in the convex annulus.

**Conclusion—**Asymmetric compression had direct deleterious effects on both tissue and cells, suggesting an injurious loading regime that could lead to a degenerative cascade, including cell death, the production of inflammatory mediators, and a shift towards catabolism. This explant



Corresponding Author: James C. Iatridis, Mount Sinai School of Medicine, One Gustave L. Levy Place, Box 1188, New York, NY 10029-6574, 212-241-1517 (office), 212-876-3168 (fax), james.iatridis@mssm.edu.

**Conflict of Interest**
The authors do not have any conflicts of interest to disclose.

**Contributions**
*Walter B.A:* Conception and design, collection, assembly and interpretation of data, drafting of article, and responsible for integrity of work.
*Korecki C.L:* Conception and design, interpretation of data, critical revision for intellectual content, final approval.
*Purmessur D:* Collection and interpretation of data, critical revision for intellectual content, final approval.
*Roughley P.J:* Collection, assembly and interpretation of data, critical revision for intellectual content, final approval.
*Michalek A.J:* Interpretation of data, critical revision for intellectual content, final approval.
*Iatridis J.C:* Conception and design, interpretation of data, critical revision for intellectual content, final approval, obtained funding.

model is useful to assess how injurious mechanical loading affects the cellular response which may contribute to the progression of degenerative changes in large animal IVDs, and results suggest that interventions should address inflammation, apoptosis, and lamellar integrity.

**Keywords**

intervertebral disc; organ culture; mechanical loading; apoptosis; catabolism

## Introduction

Mechanical factors are known to influence the biological response of intervertebral disc (IVD) tissue through altering metabolic activity and matrix integrity [1–4]. Some evidence suggests there is a threshold of mechanical loading beyond which structural damage occurs and metabolic activity shifts toward catabolic remodeling [2, 3, 5], yet it is less clear whether structural damage in the IVD is more dependent on load magnitude or loading mode. Large magnitudes of dynamic compression (up to 2.5MPa) applied to IVDs was shown to increase IVD metabolism with a slow rate of accumulation of degenerative changes [6, 7]. Torsion does not appear to be particularly damaging to the IVD as the amount of torsional rotation needed for structural failure of the human lumbar IVD (±10°) is well above the physiologic rotations experienced (±2°) [8]. In addition large magnitudes of torsion did not induce detrimental changes in biosynthetic activity or structural disruption in a rat caudal model [9], and induced rotational instability (via facet removal) in a rabbit model did not cause progressive IVD degeneration [10]. Together, results suggest that the IVD can tolerate large amounts of loading in a single loading modality.

The combination of multiple loading modes, or complex loading, develops in many spinal motions such as bending with compression. The extreme complex loading that develops in hyperflexion has long been implicated in IVD injury [11, 12] with one possible mechanism being the development of large amounts of shear strain [13, 14] in addition to the compressive axial strain. However, the propensity for less extreme complex loading to cause injury has also been documented in a study examining the combination of axial torque with flexion-extension fatigue loading and found that the loading accelerated injury and failure in porcine motion segments [15]. Biomechanical evaluations of injurious loading on the IVD determined that extreme loading can lead to herniation or other IVD pathologies with limited understanding of the corresponding biologic consequences. Improved understanding of the interaction of biomechanical and biological factors with injurious loading is required to inform effective strategies that provide functional restoration of intervertebral discs and prevent progressive degeneration.

Small animal studies documented changes in annular organization [16–18] and a region specific reduction in anabolic gene expression resulting from forced bending [16]. However, effects on the biomechanical response of the IVD tissue to forced bending remain inconclusive [16, 18] and additional measures of the corresponding catabolic response would help characterize the effects of loading on cellular metabolism. Changes in cellular and enzymatic activity as well as annular morphology have also been documented in IVDs that experience compression with bending from animal models or scoliosis [16, 17, 19–21]. Yet, the contribution of complex loading in influencing these cellular and structural changes is difficult to quantify in small animal models and difficult to separate from underlying disease processes in scoliosis.

One potential outcome of complex loading is an initiation of an inflammatory response via increases in pro-inflammatory mediators in response to abnormal tissue stress [9, 22]. Pro-inflammatory cytokines are expressed by IVD cells [23] and are known to influence cellular

metabolism, suggesting that IVD cells may be capable of inducing a localized inflammatory response. Little is known concerning the role that such an inflammatory response plays in reaction to mechanical loading but one possible consequence would be an increase in catabolic activity due to pro-inflammatory mediators [24, 25].

The aim of this study was to develop an IVD explant model of injury using hyperflexion as an example of complex loading in order to evaluate the early mechanical and biological response of IVDs to injurious loading. Improved understanding of the early response to injury will improve understanding of the role of injury (or micro-injury) in progression of disease and may also help inform the most promising treatment options. A large animal ex-vivo model was used because its cell type and size approach the human condition [26–28] and the large amount of tissue enabled concurrent measurements of the short-term mechanical and biologic responses to complex loading. It was hypothesized that the complex loading would result in structural disruption (detectable both histologically and mechanically), and an associated cellular adaptation involving a catabolic shift in protein synthesis, that is at least partly mediated by up-regulation of pro-inflammatory cytokines. This hypothesis was tested by applying axial compression asymmetrically via a 15° angulation to bovine caudal IVDs in an explant culture model. The mechanical and cellular responses were evaluated through confined compression, qRT-PCR, histology and compositional measurements including western blot to evaluate aggrecan degradation products.

## Methods

### Organ Culture Set-Up

Thirty two IVDs were harvested from 3 caudal levels (c2-3, c3-4, and c4-5) of 12 bovine tails (ages 18–24 months) obtained from a local abattoir. Isolated discs were assigned to either a Control group or a Wedge group so that from each tail one IVD was assigned to the control group and the remaining IVDs were assigned to the Wedge group. For analysis of all quantitative results the two IVDs assigned to the wedge group from each tail were averaged so that from each animal there was one control IVD and one averaged wedge IVD to provide N=12 animals per group (Appendix). IVDs from different caudal levels were systematically distributed between groups to minimize potential level effects, although it was previously reported that there were no effects of level on bovine caudal IVDs for GAG, collagen, denatured type II collagen or DNA contents and small or negligible effects on IVD water content for IVDs of this age [29]. All dissections were conducted under sterile conditions and included careful removal of endplates, after which discs were immediately rinsed in ethanol, phosphate buffered saline (PBS) containing 3% penicillin/streptomycin and 1.5% fungizone (Invitrogen, Carlsbad, CA), and PBS. Both groups were cultured for 7 days to allow for cellular adaptation at both the gene and protein level and loaded with 0.2 MPa baseline static compression, previously shown to be an appropriate baseline loading condition for this culture system [27]. Wedge specimens were cultured in a modified chamber that applied baseline compressive load at a prescribed 15° angle (Figures 1a) while control specimens were uniformly loaded with the baseline compressive load alone. The convex and concave sides of each wedged disc (Figure 1b) were analyzed for all dependent variables. The loading conditions were chosen to induce injury but fall within the high end of physiological conditions while also allowing a reproducible loading regime in a previously established culture system. The 15° angulation is within the range observed in scoliotic spines [30], and a pilot study using a hexapod [31] demonstrated the angulation induced a shear force approximately 25% of axial force which is a similar proportion to that found in vivo in humans during asymmetric lifting exertions [32]. To additionally characterize the stress state of the tissue the axial stress distribution was assessed using

LLLW Fuji Prescale Film (Tekscan, South Boston, MA) following manufacturer instructions (Control N=2, Wedge N=2).

### Structure & Composition

To evaluate whether any changes in matrix integrity occurred multiple structural parameters were assessed. IVD height and diameter were recorded at the set up and take down of the experiment. Media was collected at days 4 and 7 of the culture and used to analyze glycosaminoglycan (GAG) content released into the culture media through dimethyl methylene blue (DMMB) colorimetric assay [33] (Control N=12; Wedge N=12) and normalized to the initial volume of the intact IVD (calculated from initial dimensions). To characterize how AF disruption influenced aggrecan content and structure, AF tissue (taken adjacent from mechanical testing specimens) was analyzed for protein level changes in aggrecan content (Control N=2; Wedge N=2) using western blot analysis as previously described [34]. Water content was calculated from samples of AF tissue collected from the two sides of the IVD (Control N=6; Wedge N=6) following tissue dissection, weighing and lyophilization. A sagittal section of tissue was fixed in 10% formalin for 7–10 days, paraffin embedded, sectioned and stained using picrosirius red and alcian blue (Sigma Aldrich) to examine tissue structure (Control N=6; Wedge N=6) [35].

### Tissue Mechanics

To characterize how structural disruption impacted the mechanical behavior of the AF the mechanical properties were assessed through stress relaxation tests in confined compression on Control (N=6) and Wedge specimens (N=6). IVDs used for mechanical assessment were flash frozen and stored at −20°C until testing. Frozen IVD's were divided in half reflecting the concave or convex halves or opposing sides of the control and microtomed to a thickness of 1.0±0.08 mm after which a 5.0mm-diameter plug was taken from the AF of each half with a biopsy punch (Figure 2). Confined compression stress relaxation experiments were performed as previously described [36]. Aggregate modulus ($H_A$) was calculated from the slope of the equilibrium stress-strain plots using a linear approximation ($R^2$ >0.99) and peak stress/equilibrium stress ratio was calculated at 15% strain to assess relative viscoelastic contributions.

### Gene Expression

To evaluate any changes to cellular metabolism, qRT-PCR was performed on tissue isolated from the AF and NP regions of control (N=6) and both concave and convex sides of the wedged (N=6) IVDs. Briefly, tissue was dissected using a custom dissection tool that cut ~4mm wide strips on either side of the center of the IVD. The AF and NP regions were separated and the inner AF was discarded. The tissue was then flash frozen in liquid nitrogen, pulverized and mRNA was extracted using the Qiagen RNEasy Kit (Qiagen, USA). Gene expression levels were quantified using SYBR green (Applied Biosystems, CA) bovine specific primers for aggrecan, collagen types I and II, ADAMTS-4, and MMP-1 target genes and the house-keeping 18S rRNA. The AF region was additionally assessed for expression of pro-inflammatory cytokines TNFα, IL-1β, and IL-6. All primers except IL-6 were previously designed and validated [37, 38]. IL-6 was designed using Beacon software with the following sequence: IL-6 Forward; CCA-GGA-ACG-AAA-GAG-AGC Reverse; GGA-GTG-GTC-AGA-AGT-AGT-C with Ta of 60°C and Tm of 84°C. All target gene expression levels were analyzed using the comparative $\Delta\Delta C_T$ method and normalized to 18S expression levels and to tail-matched controls, as described by Livak et al. [39].

### Cell Viability/Apoptosis

To evaluate if cells died in response to the altered loading and lamellar disruption, viability and apoptosis were measured. Cell viability was assessed (Control N=3; Wedge N=3) using 3-(4,5-dimethylthiazol-2-yl)-2,5-diphenyltetrazolium bromide (MTT, Sigma-Aldrich, St. Louis, MO) which stains viable cells [27], and 4′,6-diamidino-2-phenylindole (DAPI, Roche Diagnostics, Germany) which stains the nuclei of all cells. Cells double stained for DAPI and MTT were viable, and those with DAPI without MTT were nonviable. Following culture, full diameter tissue sections were dissected in the sagittal plane of the disc and placed into PBS containing 1mg/mL MTT for 3 hours. Tissue was washed, flash frozen and stored at −80°C until sectioning on a cryotome. Three 10μm thick sections were taken from each disc, beginning at the tissue surface and every 100μm thereafter. Slides were fixed with 10% formalin, counter-stained with DAPI, and cover slipped. Representative images were captured at 20x magnification first under fluorescent light to capture cell nuclei stained with DAPI (Ultraviolet filter) and then under bright field light to capture vital cells stained with MTT; the images were then merged. The total number of cells (DAPI) and dual stained cells (DAPI+MTT) were counted using ImageJ (National Institutes of Health, Bethesda, MD) and a viability percentage [Live (MTT+DAPI)/Total (DAPI)] was calculated for each image.

Apoptosis was assessed using immunofluorescence for caspase-3 and performed as previously described [40] on both control (N=2) and wedge (N=2) samples. A primary rabbit anti-bovine polyclonal cleaved caspase-3 antibody (1:250 dilution, Catalog #9661S; Cell Signaling Technology, Boston, MA) and goat anti-rabbit secondary antibody (2mg/mL, Alexa 555; Invitrogen, Carlsbad, CA) were applied. Positive controls (mouse thymus treated with dexamethasone) and negative controls (omission of primary antibody) were included in the experiment. Representative images were captured at 25x magnification on a confocal microscope (Zeiss LSM 510).

### Statistical Analysis

All results were assessed for normality using a Ryan-Joiner normality test. A repeated-measures ANOVA with a Tukey post hoc test was used to evaluate the effects of complex loading on structural and compositional measurements comparing control, concave and convex conditions. A one-way ANOVA (non-repeated measures) was used for mechanical testing since four data points from different tails were not collected due to technical issues during the testing (the actuator became unstable since we ‘tuned’ the actuator on the control tissue but stiffness of concave and convex samples were substantially different). A paired t-test compared GAG released into media between wedge and control groups. For qRT-PCR, one sample t-tests were done on the $\Delta\Delta C_T$ values to assess differences from control ($\Delta\Delta C_T=0$) and paired t-tests were done to determine difference between concave and convex sides. All values are reported as average (95% confidence interval). All statistical analysis were conducted with GraphPad Prism 3 (La Jolla, CA) with $p<0.05$ considered significant.

## Results

### Structure & Composition

There was a significant increase in water content ($p=0.0016$) on the convex side 68.9% (66.7–71.1%) of the wedged IVDs compared to concave side 64.8% (62.8–66.7%) and compared to the control 63.8% (60.7–66.8%). There were no significant differences between the changes in disc diameters in all groups. There were significant differences in disc height compared to control ($p<0.0001$); the control decreased on average 38.1% (31.1–45.1%), the concave side decreased on average 74.1% (70.2–78.1%), and the convex side decreased on average 5.4% (4.5-increase 15.4%). There were no significant differences in GAG released to media between control and wedge groups at any time point. Western blot analysis showed

a lower content of aggrecan core proteins including degraded aggrecan fragments in the concave side of wedged IVDs compared to control while the convex side was similar to control (Figure 3). Annular disruption and NP migration were observed histologically in the wedge loaded group compared to the control group and the concave AF of the wedged IVDs showed lamellar buckling while the convex annulus appeared to show a limited increase in proteoglycan staining (Figure 4).

### Tissue Mechanics

The Fuji Prescale Film analysis demonstrated the 15° angulation induced a repeatable axial stress distribution (Figure 1c) with control IVDs experiencing a uniform stress distribution (~0.23MPa) and the wedged IVDs experiencing an axial stress of up to ~0.45MPa in concave AF regions and ~0.23MPa or less in convex AF regions. For confined compression the concave AF exhibited the highest aggregate modulus which was significantly different from the convex side ($p=0.033$) and trended higher than the control (Table 1). The confined compression peak stress/equilibrium stress on the convex side was significantly greater than the concave side ($p=0.013$) and trended greater than the control.

### Gene Expression

When examining changes at the gene expression level, no significant changes were observed in the NP of wedge loaded IVDs compared to control (data not shown). In the convex AF of wedged IVDs, MMP-1 (3.2 fold), ADAMTS4 (3.8 fold), IL-1β (3.8-fold), and IL-6 (2.8-fold) mRNAs were significantly up-regulated compared to control (Table 2). There were significant differences in MMP-1 ($p=0.04$) and ADAMTS4 ($p=0.005$) gene expression between the concave and convex sides of the wedged discs. TNFα was not consistently expressed in any sample.

### Cell Viability/Apoptosis

There was consistent nuclear staining (DAPI) in all regions of all IVDs, demonstrating a uniform presence of cell nuclei in the tissue. Control tissue contained no regional differences in live cell staining with 83.8% (71.6–95.9%) tissue viability in the AF. However, wedge tissue exhibited a disparity in live cell staining ($p=0.005$) (MTT+DAPI) with a significant decrease in tissue viability of the concave AF (13.2% (0–57.1%)) compared to control while the convex AF (77.6% (18.0–100%)) was similar to control (Figure 5a). No differences in viability were observed between the NP of all groups. To probe the potential mechanism of cell death a small subset of wedge and control IVDs were analyzed for caspase-3, an apoptosis specific protein. Greater caspase-3 staining was observed on the concave side compared to the convex side of the wedged IVD and compared to the control. Some sparse caspase-3 staining was present in the convex AF and in one of the controls (Figure 5b).

## Discussion

This study investigated how complex loading via asymmetric compression affects the tissue and cellular response of the IVD, to test the hypothesis that complex mechanical loading can lead to IVD injury, detectable mechanically and cellularly. Asymmetric compression was found to be injurious throughout the tissue affecting IVD cellular biology and the structural integrity. At the cellular level there was a loss of viable cells via apoptosis in the concave annulus and an up-regulation of both catabolic and pro-inflammatory cytokine mRNA expression in the convex annulus. At the tissue level, there was annular disruption evident through altered histology, tissue compaction, decreased viscoelastic responses, and some evidence of aggrecan loss. The most notable finding was the extent of injury resulting from low magnitudes of axial compression applied at high levels of angulation which strongly

contrasts loading in a single modality [7] and is likely to be associated with shear-induced structural disruption to the tissue matrix.

The removal of endplates was necessary to maintain cell viability in this organ culture model [41], although the extent of the resulting structural disruption was likely greater than would be expected in-vivo. The injurious response observed in this study with compression magnitudes of only 0.2 MPa strongly contrasted a prior study that also removed vertebral endplates and found that IVDs subjected to dynamic compression (up to 2.5 MPa) increased biosynthesis without evidence of structural disruption or cell death [7]. This comparison reinforces the concept that asymmetric compression leads to injury on cellular and structural levels, while dynamic compression was suggestive of a healthy loading condition for the IVD [6, 7]. The static baseline load has been used previously [27], and may reduce biosynthesis rates but should not affect comparison relative to control and was considered a reasonable baseline condition in this study. The applied angulation is similar to that found in scoliosis so that relative changes in disc height from concave to convex sides is similar to that found in scoliotic spines. However, the change in disc height for both control and wedge groups is larger than expected compared to the in vivo situation and is likely due increased bulging related to endplate removal and postmortem muscle relaxation/swelling prior to the start of culture.

The decrease in cellular viability observed in the concave AF was the most dramatic cellular response to the altered loading. This is consistent with findings in scoliotic tissue where DNA levels were significantly lower in the concave annulus as well with other small animal bending models [16, 19, 42]. The increased caspase-3 staining in the concave AF suggests that the observed cell death is mediated through apoptosis and is consistent with other small animal models that showed TUNEL staining in the concave AF of murine caudal IVDs subjected to static bending [16].

While asymmetric compression induced cell death in the concave annulus the altered loading also provoked an inflammatory response with significant up-regulation of mRNA for pro-inflammatory cytokines IL-1β and IL-6 in the convex annulus. IL-1β has been strongly associated with matrix degradation through the up regulation of both mRNA and activation of MMP levels in the IVD [43–45], suggesting that the increase in IL-1β observed here may have contributed to the observed increase in MMP-1. TNFα has been implicated in the initiation of the inflammatory response with downstream up-regulation of IL-1 [44]; hence, observing no changes in TNFα expression at 7 days may be due to the endpoint assessment missing earlier expression. This disc-specific inflammatory response is particularly interesting in the absence of any systemically mediated processes, and when taken with another study demonstrating increases in pro-inflammatory mRNA in response to torsion [9], may suggest a cellular sensitivity to shear loading leading to pro-inflammatory cytokine expression.

Structural disruption in the AF was evident through changes in water and GAG content and also mechanical properties. The increase in aggregate modulus of the concave AF implies that tissue compaction occurred and would suggest a decrease in permeability (i.e., an increase in peak to equilibrium stresses). However, the opposite was observed, and the concave side was shown to have a decreased peak to equilibrium stress suggesting that structural disruption from asymmetric compression may increase water transport. Water transport within the AF that occurs in the axial direction is thought to be via microtubules oriented parallel to the collagen fibers [46] and the increase in axial water transport in this study may result from microtubules parallel to the direction of the compaction becoming enlarged due to the Poisson effect, which is consistent with histology where the AF was compacted axially (loss of height) and was stretched laterally (NP shift). Furthermore, the

suggestion of increased water transport possibly via increased porosity on the concave side would suggest that the observed increase in apoptosis-mediated cell death was independent of nutritional compromise.

On the convex side, reductions in aggregate modulus contrast increased peak to equilibrium stresses. The reduced modulus is likely associated with the increased water content observed. The increased peak to equilibrium stress suggests reduced water transport that may be associated with an increase in GAG present in the convex AF which was suggested histologically via NP migration towards the convex side and is consistent with scoliotic literature where the NP migrates towards the convexity and increased proteoglycan content in the convex AF has been reported [19, 47].

This study reinforces the previously established concept of mechanically induced cell death [48, 49] and highlights the role of apoptosis rather than necrosis as the likely mechanism. However, the amount of cell death resulting from the modest axial compressive stress in the concave AF (~0.45MPa) observed in this study contrasts a previous study that used an in vivo murine tail model and observed limited cell death in IVDs that experienced a uniform compressive stress (0.4MPa) for the same duration, suggesting that magnitude of axial stress alone may have a limited contribution to the amount of cell death in the present study. Previous work has suggested that the large shear strains that develop when compression is combined with flexion/extension place the disc at risk of structural injury [13] and when taken with the large amounts of cell death in the concave annulus observed in this and other bending studies [16, 42] may suggest that shear strains resulting from asymmetric compression influence the degree of cellular injury more than compression alone. However removal of endplates in this study is likely to increase the amount of shear strains compared to endplate-retaining models.

In conclusion, complex loading consisting of axial compression at an applied 15° angulation, was investigated in a large animal organ culture model. Asymmetric compression was injurious even at low magnitudes of force, inducing cell death, structural disruption, and an increase in catabolic and pro-inflammatory cytokine mRNA production, suggestive of a degenerative cascade. This model is useful to assess how the mechanobiology associated with injurious loading may contribute to the progression of degenerative changes and how potential treatments may help slow these processes. These injurious conditions are likely associated with increased tissue shear strains resulting from the asymmetric compression input. Findings also suggest the most promising opportunities for intervention involve limiting cell death associated with structural disruption and reducing the pro-inflammatory cytokine expression in response to injury. We infer that asymmetric, or wedge loading that occurs in multiple spinal pathologies affecting posture can induce aberrant cell mediated responses in the absence of underlying disease or nutritional compromise so that injurious mechanical loading may contribute to biological disruptions associated with IVD pathologies in addition to the known structural derangement. Future work may elucidate how early interventions can mitigate IVD injuries.

## Supplementary Material

Refer to Web version on PubMed Central for supplementary material.

## Acknowledgments

The authors would like to acknowledge the technical and logistical contributions of Karolyn Godburn, and Amanda Machamer. This study was sponsored by NIH grant (R01AR051146), NASA/Vermont Space Grant Consortium (NNX07AK92A) and AO Research Fund (project F-09-10I) of the AO Foundation.

## References


1. Iatridis JC, MacLean JJ, Roughley PJ, Alini M. Effects of mechanical loading on intervertebral disc metabolism in vivo. J Bone Joint Surg Am. 2006; 88 (Suppl 2):41–6. [PubMed: 16595442]
2. Stokes IA, Iatridis JC. Mechanical conditions that accelerate intervertebral disc degeneration: overload versus immobilization. Spine (Phila Pa 1976). 2004; 29:2724–32. [PubMed: 15564921]
3. Walsh AJ, Lotz JC. Biological response of the intervertebral disc to dynamic loading. J Biomech. 2004; 37:329–37. [PubMed: 14757452]
4. Hsieh AH, Twomey JD. Cellular mechanobiology of the intervertebral disc: new directions and approaches. J Biomech. 43:137–45. [PubMed: 19828150]
5. Maclean JJ, Lee CR, Alini M, Iatridis JC. Anabolic and catabolic mRNA levels of the intervertebral disc vary with the magnitude and frequency of in vivo dynamic compression. J Orthop Res. 2004; 22:1193–200. [PubMed: 15475197]
6. Wuertz K, Godburn K, MacLean JJ, Barbir A, Donnelly JS, Roughley PJ, et al. In vivo remodeling of intervertebral discs in response to short- and long-term dynamic compression. J Orthop Res. 2009; 27:1235–42. [PubMed: 19274755]
7. Korecki CL, MacLean JJ, Iatridis JC. Dynamic compression effects on intervertebral disc mechanics and biology. Spine (Phila Pa 1976). 2008; 33:1403–9. [PubMed: 18520935]
8. Adams MA, Hutton WC. The relevance of torsion to the mechanical derangement of the lumbar spine. Spine (Phila Pa 1976). 1981; 6:241–8. [PubMed: 7268544]
9. Barbir A, Godburn KE, Michalek AJ, Lai A, Monsey RD, Iatridis JC. Effects of Torsion on Intervertebral Disc Gene Expression and Biomechanics, Using a Rat Tail Model. Spine (Phila Pa 1976).
10. Stokes IA, Counts DF, Frymoyer JW. Experimental instability in the rabbit lumbar spine. Spine (Phila Pa 1976). 1989; 14:68–72. [PubMed: 2913671]
11. Adams MA, Hutton WC. Prolapsed intervertebral disc. A hyperflexion injury 1981 Volvo Award in Basic Science. Spine (Phila Pa 1976). 1982; 7:184–91. [PubMed: 7112236]
12. Adams MA, Roughley PJ. What is intervertebral disc degeneration, and what causes it? Spine (Phila Pa 1976). 2006; 31:2151–61. [PubMed: 16915105]
13. Costi JJ, Stokes IA, Gardner-Morse M, Laible JP, Scoffone HM, Iatridis JC. Direct measurement of intervertebral disc maximum shear strain in six degrees of freedom: motions that place disc tissue at risk of injury. J Biomech. 2007; 40:2457–66. [PubMed: 17198708]
14. Michalek AJ, Buckley MR, Bonassar LJ, Cohen I, Iatridis JC. Measurement of local strains in intervertebral disc anulus fibrosus tissue under dynamic shear: contributions of matrix fiber orientation and elastin content. J Biomech. 2009; 42:2279–85. [PubMed: 19664773]
15. Drake JD, Aultman CD, McGill SM, Callaghan JP. The influence of static axial torque in combined loading on intervertebral joint failure mechanics using a porcine model. Clin Biomech (Bristol, Avon). 2005; 20:1038–45.
16. Court C, Colliou OK, Chin JR, Liebenberg E, Bradford DS, Lotz JC. The effect of static in vivo bending on the murine intervertebral disc. Spine J. 2001; 1:239–45. [PubMed: 14588327]
17. Stokes, I.; McBride, CA.; Aronsson, DD.; Roughley, PJ. Intervertebral disc changes in an animal model representing altered mechanics in scoliosis. Abstract. 55th Annual Meeting of the Orthopaedic Research Socitey; Las Vegas, NV. 2009.
18. Stokes IA, McBride CA, Aronsson DD. Intervertebral disc changes in an animal model representing altered mechanics in scoliosis. Abstract Stud Health Technol Inform. 2008; 140:273–7.
19. Crean JK, Roberts S, Jaffray DC, Eisenstein SM, Duance VC. Matrix metalloproteinases in the human intervertebral disc: role in disc degeneration and scoliosis. Spine (Phila Pa 1976). 1997; 22:2877–84. [PubMed: 9431623]
20. Roberts S, Menage J, Eisenstein SM. The cartilage end-plate and intervertebral disc in scoliosis: calcification and other sequelae. J Orthop Res. 1993; 11:747–57. [PubMed: 8410475]
21. Bertram H, Steck E, Zimmerman G, Chen B, Carstens C, Nerlich A, et al. Accelerated intervertebral disc degeneration in scoliosis versus physiological ageing develops against a

background of enhanced anabolic gene expression. Biochem Biophys Res Commun. 2006; 342:963–72. [PubMed: 16598853]

22. Lotz JC, Ulrich JA. Innervation, inflammation, and hypermobility may characterize pathologic disc degeneration: review of animal model data. J Bone Joint Surg Am. 2006; 88 (Suppl 2):76–82. [PubMed: 16595449]
23. Burke JG, Watson RW, McCormack D, Dowling FE, Walsh MG, Fitzpatrick JM. Spontaneous production of monocyte chemoattractant protein-1 and interleukin-8 by the human lumbar intervertebral disc. Spine (Phila Pa 1976). 2002; 27:1402–7. [PubMed: 12131736]
24. Le Maitre CL, Freemont AJ, Hoyland JA. The role of interleukin-1 in the pathogenesis of human intervertebral disc degeneration. Arthritis Res Ther. 2005; 7:R732–45. [PubMed: 15987475]
25. Seguin CA, Pilliar RM, Roughley PJ, Kandel RA. Tumor necrosis factor-alpha modulates matrix production and catabolism in nucleus pulposus tissue. Spine (Phila Pa 1976). 2005; 30:1940–8. [PubMed: 16135983]
26. Alini M, Eisenstein SM, Ito K, Little C, Kettler AA, Masuda K, et al. Are animal models useful for studying human disc disorders/degeneration? Eur Spine J. 2008; 17:2–19. [PubMed: 17632738]
27. Korecki CL, MacLean JJ, Iatridis JC. Characterization of an in vitro intervertebral disc organ culture system. Eur Spine J. 2007; 16:1029–37. [PubMed: 17629763]
28. Oshima H, Ishihara H, Urban JP, Tsuji H. The use of coccygeal discs to study intervertebral disc metabolism. J Orthop Res. 1993; 11:332–8. [PubMed: 8326439]
29. Demers CN, Antoniou J, Mwale F. Value and limitations of using the bovine tail as a model for the human lumbar spine. Spine (Phila Pa 1976). 2004; 29:2793–9. [PubMed: 15599281]
30. Rajasekaran S, Vidyadhara S, Subbiah M, Kamath V, Karunanithi R, Shetty AP, et al. ISSLS Prize Winner: A Study of Effects of In Vivo Mechanical Forces on Human Lumbar Discs With Scoliotic Disc as a Biological Model: Results From Serial Postcontrast Diffusion Studies, Histopathology and Biochemical Analysis of Twenty-One Human Lumbar Scoliotic Discs. Spine (Phila Pa. 1976; 35:1930–43.
31. Stokes IA, Gardner-Morse M, Churchill D, Laible JP. Measurement of a spinal motion segment stiffness matrix. J Biomech. 2002; 35:517–21. [PubMed: 11934421]
32. Marras WS, Ferguson SA, Burr D, Davis KG, Gupta P. Spine loading in patients with low back pain during asymmetric lifting exertions. Spine J. 2004; 4:64–75. [PubMed: 14749195]
33. Farndale RW, Buttle DJ, Barrett AJ. Improved quantitation and discrimination of sulphated glycosaminoglycans by use of dimethylmethylene blue. Biochim Biophys Acta. 1986; 883:173–7. [PubMed: 3091074]
34. Haglund L, Ouellet J, Roughley P. Variation in chondroadherin abundance and fragmentation in the human scoliotic disc. Spine (Phila Pa 1976). 2009; 34:1513–8. [PubMed: 19525844]
35. Korecki CL, Costi JJ, Iatridis JC. Needle puncture injury affects intervertebral disc mechanics and biology in an organ culture model. Spine (Phila Pa 1976). 2008; 33:235–41. [PubMed: 18303454]
36. Perie D, Korda D, Iatridis JC. Confined compression experiments on bovine nucleus pulposus and annulus fibrosus: sensitivity of the experiment in the determination of compressive modulus and hydraulic permeability. J Biomech. 2005; 38:2164–71. [PubMed: 16154403]
37. Wuertz K, Urban JP, Klasen J, Ignatius A, Wilke HJ, Claes L, et al. Influence of extracellular osmolarity and mechanical stimulation on gene expression of intervertebral disc cells. J Orthop Res. 2007; 25:1513–22. [PubMed: 17568421]
38. Fitzgerald JB, Jin M, Grodzinsky AJ. Shear and compression differentially regulate clusters of functionally related temporal transcription patterns in cartilage tissue (Supplemental Material). J Biol Chem. 2006; 281:24095–103. [PubMed: 16782710]
39. Livak KJ, Schmittgen TD. Analysis of relative gene expression data using real-time quantitative PCR and the 2(−Delta Delta C(T)) Method. Methods. 2001; 25:402–8. [PubMed: 11846609]
40. Taatjes DJ, Wadsworth MP, Zaman AK, Schneider DJ, Sobel BE. A novel dual staining method for identification of apoptotic cells reveals a modest apoptotic response in infarcted mouse myocardium. Histochem Cell Biol. 2007; 128:275–83. [PubMed: 17684755]
41. Lee CR, Iatridis JC, Poveda L, Alini M. In vitro organ culture of the bovine intervertebral disc: effects of vertebral endplate and potential for mechanobiology studies. Spine (Phila Pa 1976). 2006; 31:515–22. [PubMed: 16508544]

42. Court C, Chin JR, Liebenberg E, Colliou OK, Lotz JC. Biological and mechanical consequences of transient intervertebral disc bending. Eur Spine J. 2007; 16:1899–906. [PubMed: 17701429]
43. Hoyland JA, Le Maitre C, Freemont AJ. Investigation of the role of IL-1 and TNF in matrix degradation in the intervertebral disc. Rheumatology (Oxford). 2008; 47:809–14. [PubMed: 18397957]
44. Millward-Sadler SJ, Costello PW, Freemont AJ, Hoyland JA. Regulation of catabolic gene expression in normal and degenerate human intervertebral disc cells: implications for the pathogenesis of intervertebral disc degeneration. Arthritis Res Ther. 2009; 11:R65. [PubMed: 19435506]
45. Shen B, Melrose J, Ghosh P, Taylor F. Induction of matrix metalloproteinase-2 and -3 activity in ovine nucleus pulposus cells grown in three-dimensional agarose gel culture by interleukin-1beta: a potential pathway of disc degeneration. Eur Spine J. 2003; 12:66–75. [PubMed: 12592549]
46. Travascio F, Jackson AR, Brown MD, Gu WY. Relationship between solute transport properties and tissue morphology in human annulus fibrosus. J Orthop Res. 2009; 27:1625–30. [PubMed: 19489044]
47. Perie D, Sales de Gauzy J, Curnier D, Hobatho MC. Intervertebral disc modeling using a MRI method: migration of the nucleus zone within scoliotic intervertebral discs. Magn Reson Imaging. 2001; 19:1245–8. [PubMed: 11755736]
48. Lotz JC, Chin JR. Intervertebral disc cell death is dependent on the magnitude and duration of spinal loading. Spine (Phila Pa 1976). 2000; 25:1477–83. [PubMed: 10851095]
49. Rannou F, Lee TS, Zhou RH, Chin J, Lotz JC, Mayoux-Benhamou MA, et al. Intervertebral disc degeneration: the role of the mitochondrial pathway in annulus fibrosus cell apoptosis induced by overload. Am J Pathol. 2004; 164:915–24. [PubMed: 14982845]

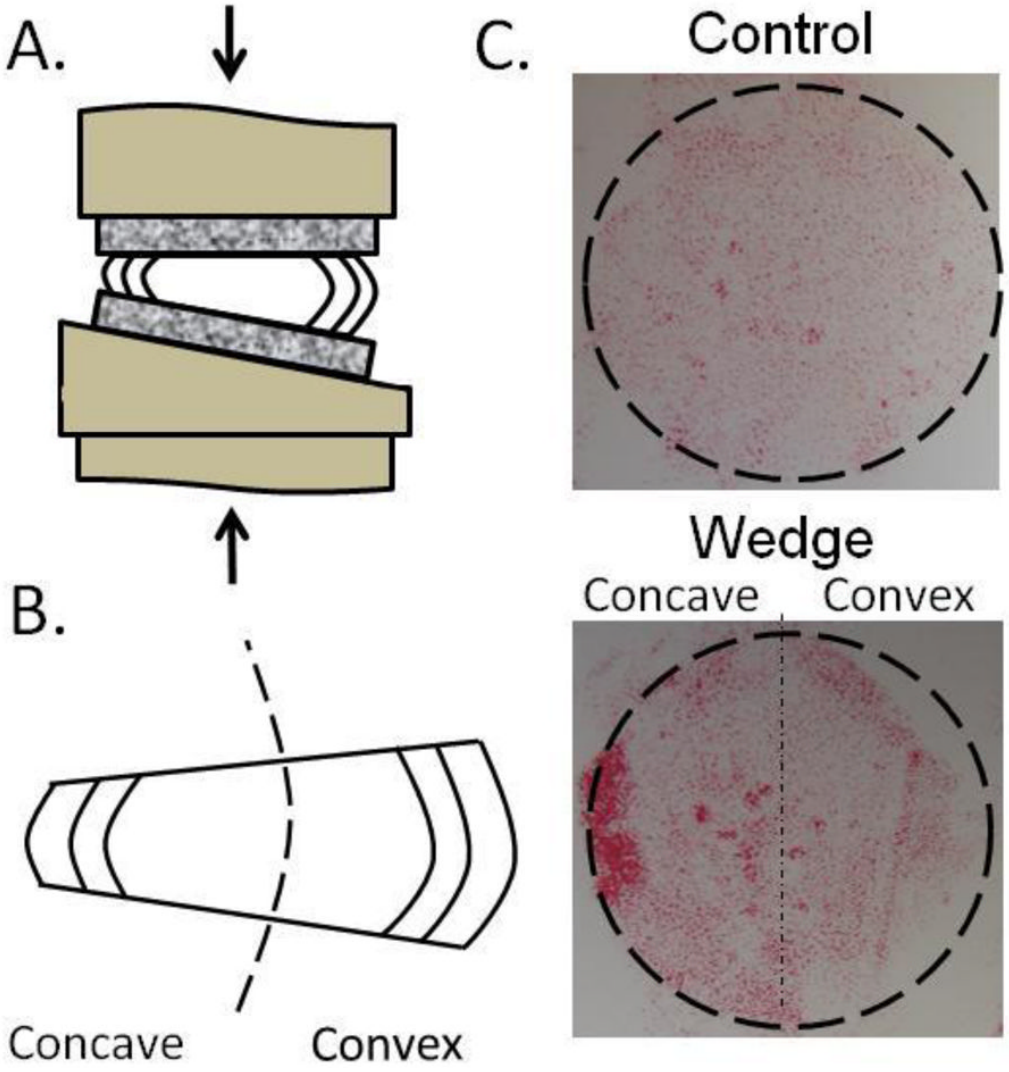


**Figure 1.**
A. Loading schematic. B. Concave/Convex nomenclature. C. Compressive stress distribution of both groups with a maximum compressive stress of ~0.45 MPa in the concave annulus.

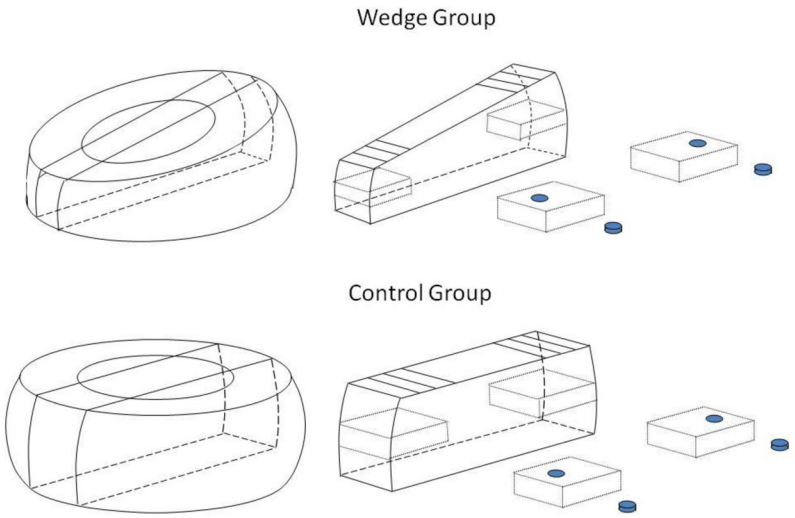


**Figure 2.**
Mechanical testing specimen preparation protocol. One specimen was taken from both side of each disc, and used for confined compression testing.

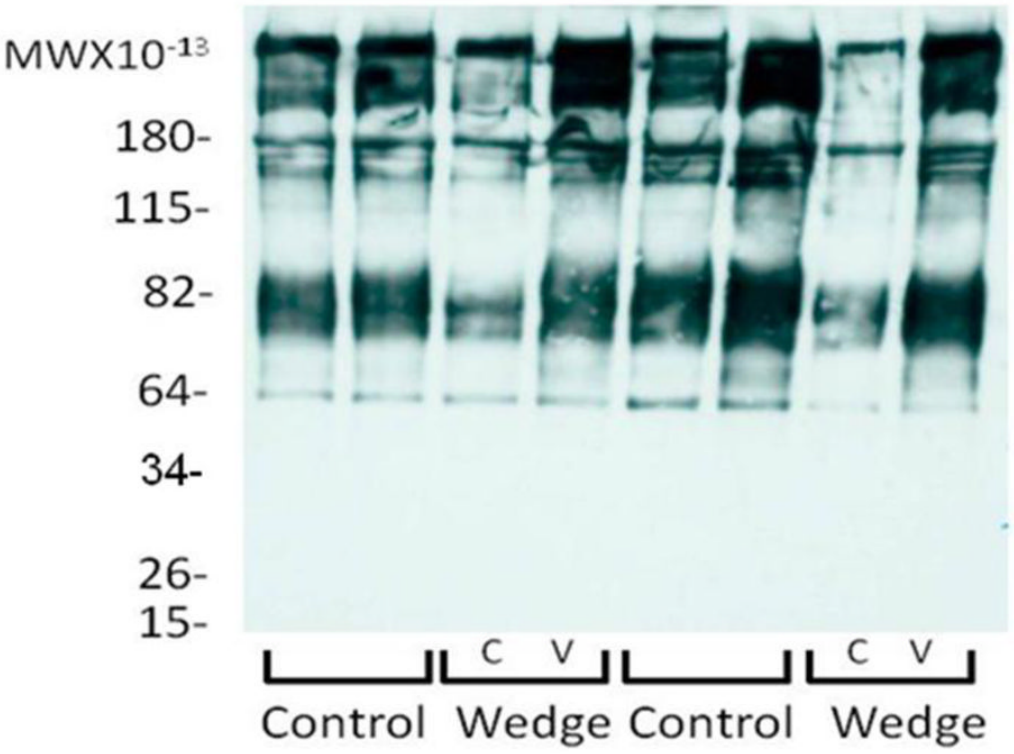


**Figure 3.**
Western blot analysis of aggrecan fragmentation demonstrating a loss of aggrecan on the concave side of wedged IVDs. C=Concave and V=Convex.

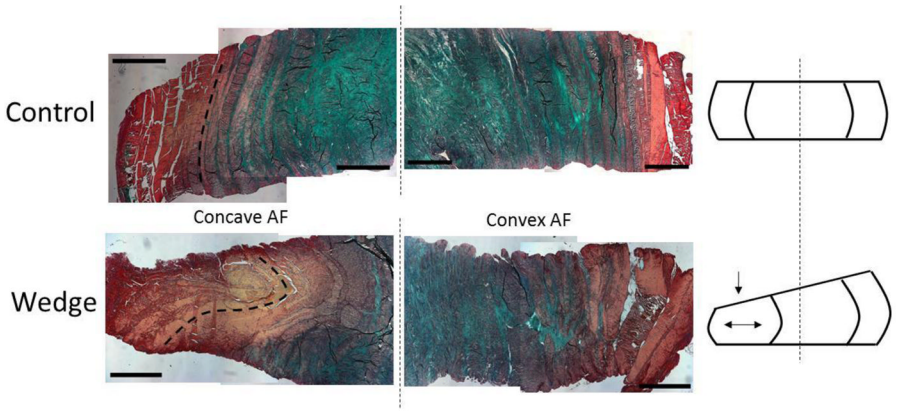


**Figure 4.**

Representative histology images of structural changes in the inner and outer annulus in control discs (top) and wedged discs (bottom). Dashed lines highlight lamellar structure demonstrating intact lamellae in control and lamellar buckling in wedged discs. Tissue compaction and a shift of the nucleus pulposus also occurred in wedged discs as seen in the schematic. Tissue has been stained with picrosirius red (collagen) and alcian blue (proteoglycans). Images were taken at 2.5x mag, scale bars represent 1000μm.

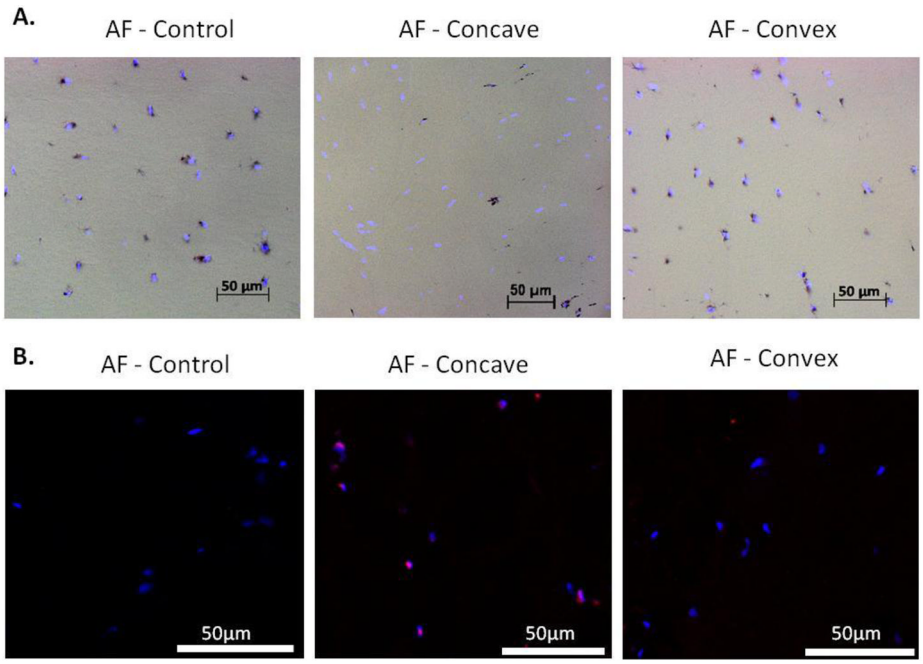


**Figure 5.**

A. Tissue viability images of outer AF for control (left) and the concave (middle) and convex (right) sides of the wedged IVD. Live cells are black (MTT), cell nuclei are fluorescent blue (DAPI). B. Caspase-3 immunofluorescence images showing more apoptosis on the concave side of the IVD. Caspase-3 positive cells stain orange and appear purple with the nuclear stain. Scale bar represents 50µm.

## Table 1

Confined Compression Mechanical Parameters. Aggregate Modulus ($H_A$) and Peak to Equilibrium ratio (P/E) at 15% strain. 95% Confidence interval denoted in ( ).

| | N | $H_A$ (MPa) | P/E |
|---|---|---|---|
| Control | 5 | 1.098 (0.521–1.676) | 3.449 (3.102–3.797) |
| Concave | 5 | 1.708 (0.464–2.951)[A] | 2.342 (1.537–3.147)[B] |
| Convex | 4 | 0.334 (0.182–0.487)[A] | 4.418 (2.155–6.680)[B] |

[A] Significantly different pair, p=0.033

[B] Significantly different pair, p=0.013

**Table 2**

Gene expression in the AF expressed as fold change relative to 18S and control levels. Average (95% CI) for anabolic (Aggrecan, Collagen types I and II), catabolic (MMP-1, ADAMTS-4), and pro-inflammatory cytokines (IL-1β and IL-6).

| | N | Aggrecan | Collagen 1 | Collagen 2 | MMP 1 | ADAMTS4 | IL-1B | IL-6 |
|---|---|---|---|---|---|---|---|---|
| Concave | 6 | 1.5 (0.4–4.4) | 1.8 (0.4–7.2) | 2.2 (0.4–8.3) | 1.1 (0.4–4.2)*A* | 1.2 (0.2–6.4)*B* | 2.8 (0.2–32.2) | 1.8 (0.0–80.2) |
| Convex | 6 | 2.1 (0.7–6.4) | 1.8 (0.9–3.6) | 1.1 (0.4–3.8) | 3.2 (1.7–5.8)*1A* | 3.8 (1.2–13.7)*2B* | 3.8 (1.5–9.8)*3* | 2.8 (1.6–5.0)*4* |

*1* p=0.005

*2* p=0.035

*3* p=0.025

*4* p=0.015

*A* p=0.04

*B* p=0.004